Progress In Electromagnetics Research M, Vol. 113, 1–10, 2022

Electromagnetic Wave Propagation through Stratified Lossy Conductive Media

Igor I. Smolyaninov[1, 2, *] and Alexander B. Kozyrev[3]

Abstract—It is commonly believed that electromagnetic waves cannot propagate in lossy conductive media and that they quickly decay inside such media over short length scales of the order of the so-called skin depth. Here we prove that this common belief is incorrect if the conductive medium is stratified. We demonstrate that electromagnetic waves in stratified lossy conductive media may have propagating character and that the propagation length of such waves may be considerably larger than the skin depth in homogeneous media. Our findings have broad implications in many fields of science and engineering. They enable radio communication and imaging in such strongly lossy conductive media as seawater, various soils, plasma, and biological tissues. They also enable novel electromagnetic metamaterial designs by mediating the effect of losses on electromagnetic signal propagation in metamaterials. Our results demonstrate a new class of inherently non-Hermitian electromagnetic media with high dissipation, no gain, and no PT-symmetry, which nevertheless have almost real eigenvalue spectrum.

1. INTRODUCTION

From the point of view of electromagnetic theory, all non-magnetic media can be sorted out into two broad categories, such as transparent dielectric (or non-conductive) media, which transmit electromagnetic waves, and conductive media, which are commonly believed to disallow electromagnetic wave propagation below their plasma frequency. It is generally assumed that electromagnetic waves quickly decay inside lossy conductive media over short length scales of the order of the so-called skin depth. The goal of this paper is to prove that this common belief is incorrect if the conductive medium is stratified.

Stratification occurs naturally in many conductive media under the influence of gravity. Examples of such stratification include many underground sedimentary rocks and soils [1] (see for example Fig. 1(b)), seawater layer on top of sandy seabed, and many other terrestrial and astronomical [2] settings. Biological tissues are also often stratified into layers of different electric conductivity (for example, skull bone and grey matter [3]). Artificial stratification is also often implemented in various electromagnetic metamaterial structures, which typically exhibit very high losses [4]. Therefore, our surprising results on long-distance electromagnetic wave propagation in strongly lossy conductive media have broad implications in many fields of physics and engineering. As we will discuss below, our results also complement recent observations of loss-enhanced transmission due to PT-symmetry in non-Hermitian optical systems [5].

Let us consider solutions of the macroscopic Maxwell equations in a geometry in which a medium is non-magnetic ($B = H$), the dielectric permittivity of the medium is continuous, and it depends only on z coordinate: $\varepsilon = \varepsilon(z)$, as illustrated in Fig. 1(a). Under such conditions spatial variables in the

Received 16 June 2022, Accepted 19 August 2022, Scheduled 30 August 2022

* Corresponding author: Igor I. Smolyaninov (smoly@umd.edu).

[1] Saltenna LLC, 1751 Pinnacle Drive #600 McLean, VA 22102, USA. [2] Department of Electrical and Computer Engineering, University of Maryland, College Park, MD 20742, USA. [3] Mission Systems' Advanced Technology, Collins Aerospace, Raytheon Technologies, 400 Collins Road, Cedar Rapids, IA 52498, USA.

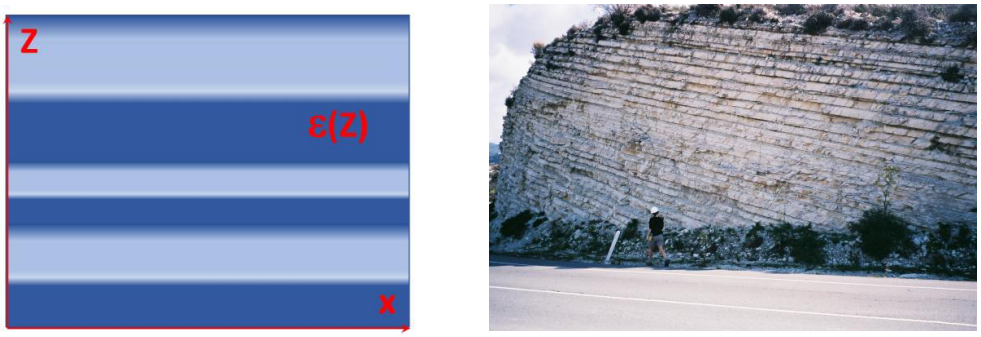

(a) (b)

Figure 1. Geometry of the problem of interest. (a) The dielectric permittivity $\varepsilon(z)$ of a bulk conductive medium is continuous and depends only on z coordinate, which is illustrated by halftones. In a strongly lossy conductive medium the dielectric permittivity is almost pure imaginary: $\varepsilon(z) \approx i\varepsilon''(z) = i\sigma(z)/\varepsilon_0\omega$. (b) Example of a conductive layered sedimentary rock.

Maxwell equations separate, and without the loss of generality we may assume electromagnetic mode propagation in the x direction, leading to field dependencies proportional to $e^{i(kx-\omega t)}$. The macroscopic Maxwell equations lead to a wave equation

$$\vec{\nabla} \times \left(\vec{\nabla} \times \vec{E} \right) = \frac{\omega^2 \varepsilon}{c^2} \vec{E} \tag{1}$$

After straightforward transformations described in detail in [3], the wave equation for the TM polarized light may be written in the form of one-dimensional Schrödinger equation

$$-\frac{\partial^2 \psi}{\partial z^2} + \left(-\frac{\varepsilon(z)\omega^2}{c^2} - \frac{1}{2}\frac{\partial^2 \varepsilon}{\varepsilon \partial z^2} + \frac{3}{4}\frac{\left(\partial\varepsilon/\partial z\right)^2}{\varepsilon^2} \right) \psi = -\frac{\partial^2 \psi}{\partial z^2} + V\psi = -k^2 \psi, \tag{2}$$

where the effective "wave function" has been introduces as $E_z = \psi/\varepsilon^{1/2}$, and the $-k^2$ term plays the role of effective energy in the Schrodinger equation. Let us consider the TM polarized solutions of Eq. (2) inside a medium having almost pure imaginary dielectric permittivity $\varepsilon(z) \approx i\varepsilon''(z) = i\sigma(z)/\varepsilon_0\omega$ where ε_0 is the dielectric permittivity of vacuum, ε'' is very large, and the medium conductivity $\sigma(z)$ is expressed in practical SI units. Based on Eq. (2), the effective potential in such a case may be written as

$$V = -\frac{i\sigma\omega}{\varepsilon_0 c^2} - \frac{1}{2}\frac{\partial^2 \sigma}{\sigma \partial z^2} + \frac{3}{4}\frac{\left(\partial\sigma/\partial z\right)^2}{\sigma^2} \tag{3}$$

The second and third terms in Eq. (3) are real, and they may become much larger than the first term if the medium conductivity changes fast enough as a function of z. Note that a more general case when the real part of $\varepsilon(z)$ in Eq. (2) is comparable to its imaginary part has been considered in [3]. It was demonstrated that the $\mathrm{Im}(V) \ll \mathrm{Re}(V)$ situation may also be realized in such a more general lossy medium case, if the loss tangent δ of the medium remains approximately constant as a function of z. In addition, since the loss tangent would remain almost constant in a multilayer structure made of such low loss plasmonic metals as gold and silver, our treatment will also be applicable in such cases. However, in order to emphasize the novel aspects of our results, let us focus our attention on the case of highly lossy multilayer materials.

2. ANALYTICAL MODEL

In general, solutions of the effective Schrodinger Eq. (2) with an effective potential $V(z)$ given by Eq. (3) must be obtained numerically [3]. However, these equations may be solved analytically for some simple spatial distributions of $\varepsilon(z)$. As an example, let us assume that $\mathrm{Re}(\varepsilon) \ll \mathrm{Im}(\varepsilon)$ and consider the

following simple parabolic spatial distribution of the dielectric permittivity inside a single conductive stratum:

$$\varepsilon(z) = A + Bz^2, \tag{4}$$

where both A and B are large imaginary coefficients, so that $a^2 = A/B$ is real and positive. These assumptions are typically valid for seawater and different ground layers in the radio frequency range [6]. The resulting effective potential for the TM electromagnetic wave is

$$V(z) \approx -\frac{4\pi^2 A}{\lambda_0^2}\left(1+\frac{z^2}{\alpha^2}\right) - \frac{1}{z^2+\alpha^2} + \frac{3z^2}{\left(z^2+\alpha^2\right)^2}, \tag{5}$$

where λ_0 is the free space wavelength. We may also introduce a notional "wavelength" inside a conductive homogeneous medium with a dielectric permittivity $\varepsilon = A$ as $\lambda = \lambda_0/\sqrt{|A|}$. The plot of $V(z)$ in the limit $\lambda \gg a$ (so that $\mathrm{Re}(V) \gg \mathrm{Im}(V)$) is shown in Fig. 2(b). We may cutoff this potential at $z = \pm\alpha/\sqrt{2}$ (and keep $\varepsilon = 1.5A$ constant at larger distances on both sides of the stratum) as illustrated in Fig. 2(a), so that the effective energy level inside such a potential well may be obtained analytically using the well-known shallow well approximation [7] as

$$k = \frac{1}{2}\int dz V(z) \approx \frac{1}{2\sqrt{2}\alpha} \tag{6}$$

(note that a 1D Schrodinger equation describing a potential well of arbitrary shape always has at least one eigenstate [7]). Let us demonstrate that the so found TM solution of Maxwell equations inside a strongly conductive absorptive medium has propagating character, and that the propagation length of such a wave may greatly exceed the skin depth.

In the limit $\varepsilon'' \gg \varepsilon'$ considered above, the conventional skin depth [6] inside a homogeneous nonmagnetic medium having $\varepsilon \approx i\varepsilon'' = A$ equals

$$\delta = \frac{1}{\sqrt{\pi\mu_0\sigma\nu}} = \frac{\lambda_0}{\pi\sqrt{2\,|A|}} = \frac{\lambda}{\pi\sqrt{2}}, \tag{7}$$

where once again we have used the fact that $\varepsilon(z) \approx i\varepsilon''(z) = i\sigma(z)/\varepsilon_0\omega$ (recall that A is imaginary). On the other hand, the propagation length L of the newly found TM wave may be obtained based on the magnitude of $\mathrm{Im}(k)$ calculated using Eqs. (5) and (6) as follows:

$$L^{-1} = \mathrm{Im}(k) \approx \frac{1}{2}\int\limits_{-\alpha/\sqrt{2}}^{\alpha/\sqrt{2}} \frac{4\pi^2 A}{\lambda_0^2}\left(1+\frac{z^2}{\alpha^2}\right)dz = \frac{14\pi^2\alpha A}{3\sqrt{2}\lambda_0^2} \tag{8}$$

As a result, the ratio L/d may be obtained as

$$\frac{L}{\delta} = \frac{3\lambda_0}{7\pi\,|A|^{1/2}\,\alpha} \approx \frac{\lambda}{7\alpha}, \tag{9}$$

which means that the TM wave propagation length may indeed be much larger than the skin depth if $\lambda \gg \alpha$. Moreover, the obtained TM wave has propagating character. Its wavelength λ_{TM} calculated as

$$\lambda_{TM} = \frac{2\pi}{\mathrm{Re}(k)} \approx 4\sqrt{2}\pi\alpha \tag{10}$$

appears much smaller than L in the $\lambda \gg \alpha$ limit:

$$\frac{L}{\lambda_{TM}} \approx \frac{3}{56\pi^2}\left(\frac{\lambda}{\alpha}\right)^2 \tag{11}$$

We should also note that Eq. (10) may be used to provide an additional straightforward justification for the fact that the propagation length of the TM wave in such a geometry may greatly exceed the skin depth. Indeed, based on Eq. (2) we may now write

$$k^2 \approx i\frac{4\pi^2}{\lambda^2} + \frac{4\pi^2}{\lambda_{TM}^2} = \frac{4\pi^2}{\lambda_{TM}^2}\left(1 + i\frac{\lambda_{TM}^2}{\lambda^2}\right), \tag{12}$$

where $\lambda_{TM} \sim \alpha \ll \lambda$. As a result,

$$k \approx \frac{2\pi}{\lambda_{TM}} \left(1 + i\frac{\lambda_{TM}^2}{2\lambda^2}\right), \tag{13}$$

which leads to $L = (\mathrm{Im}k)^{-1} \approx \lambda\frac{\lambda}{\pi\lambda_{TM}} \gg \lambda \approx \delta$. In effect, via the specified distribution of conductivity and dielectric constant we create a 2D waveguide inside a highly lossy material.

Also note that $L\lambda_{TM} \approx \lambda^2 \approx \delta^2$, which makes our results quite natural from the point of view of electromagnetic energy conservation. Anisotropic dielectric properties of the absorptive medium are supposed to deform the shape of the volume in which the electromagnetic energy is absorbed compared to the homogeneous and isotropic case, while keeping the effective volume in which the energy is absorbed approximately the same. The resulting shape is supposed to be "squeezed" along the x direction. Since we were solving a two-dimensional propagation problem in the xz plane, while disregarding the field behaviour in y-direction, the effect of medium anisotropy leads to the effective mode area conservation in the xz plane, which is exactly the result we obtained (if we note that based on Eq. (2) the field penetration in z direction approximately equals to λ_{TM}, which is considerably smaller than δ).

3. NUMERICAL SIMULATIONS

These analytical results are supported by numerical simulations shown in Fig. 2(c). The stratified conducting media (both single-well and periodic conductivity profiles) have been modeled with planar multilayer lossy dielectric structures. Wave propagation in such media have been simulated with commercial EM solver Altair Feko (www.altair.com/feko). Feko's special Green's function formulation (method of moments extension) implements 2D infinite planes with a finite thickness to model each layer of the dielectric. This simulation approach allows to verify the basic predictions of our theory, and also to illustrate that the wave propagation remains qualitatively the same in a more practical 3D case in contrast to the 1D (planar wave) formulation of our analytical theory.

Each dielectric layer of the multi-layer structure is characterized by the real part of the dielectric constant $\varepsilon_r = 1$ (the same for each layer) and by the unique conductivity σ (defining the imaginary part of the dielectric constant). The conductivity profile $\sigma(z)$ used in Figs. 2(d) and (e) is represented by a step-wise function approximating single-well parabolic dependence

$$\sigma(z) = \left(1 + 0.1z^2\right)\ \mathrm{S/m} \tag{14}$$

where z is the distance in meters. The step-wise conductivity profile has been implemented with a stack of 10 cm thick layers for $|z| < 1$ m and with 1 m thick layers for $1\,\mathrm{m} < |z| < 19\,\mathrm{m}$. The finer structure of the multilayer medium has been used near $z = 0$, since this is where most of the power flow occurs. We assumed that the medium is homogeneous for $|z| > 19$ m and its conductivity is $\sigma = 37.1\,\mathrm{S/m}$.

Electromagnetic waves have been excited by a point electric dipole with magnitude of $Idl = 1\,\mathrm{A{*}m}$ and frequency 15 kHz. The point dipole source is placed in the center of the conductive stratum (d) or inside the homogenous medium 0.5 m away from the interface with the conductive stratum (e). It is directed parallel to the layers and perpendicular to the observation plane in Figs. 2(c)–(e). Figs. 2(d) and (e) show the magnitude of the Poynting vector for the "single-well" parabolic conductivity profile. For comparison, Fig. 2(c) shows distribution of the magnitude of the Poynting vector in the medium with homogeneous conductivity $\sigma = 1\,\mathrm{S/m}$. The latter is totally defined by the skin depth which is about 4.1 m at the frequency of excitation. As one can see from Fig. 2(d), the introduction of the conductivity gradient (parabolic conductivity well) leads to generation of the surface wave confined near the center of the well and propagating in the x-y plane. Thus, the point source excites simultaneously a volumetric small-k wave (the central circle), attenuating in accordance with the skin depth prediction, and a long-propagating confined 2D mode in accordance with Eqs. (12), (13). This 2D surface wave has a TM character with electric and magnetic field structure similar to the structure of the symmetric fundamental mode of the dielectric waveguide. This wave has 2D (cylindrical) structure and attenuates much slower than a 3D spherical wave. By comparing Figs. 2(c) and (d), one can notice that the power distribution of the 3D mode in the bottom figure is squeezed in z-direction. This is because of larger effective conductivity of the stratified medium in comparison with homogeneous medium. In complete agreement with the analytical theory, it is evident that introduction of the conductivity

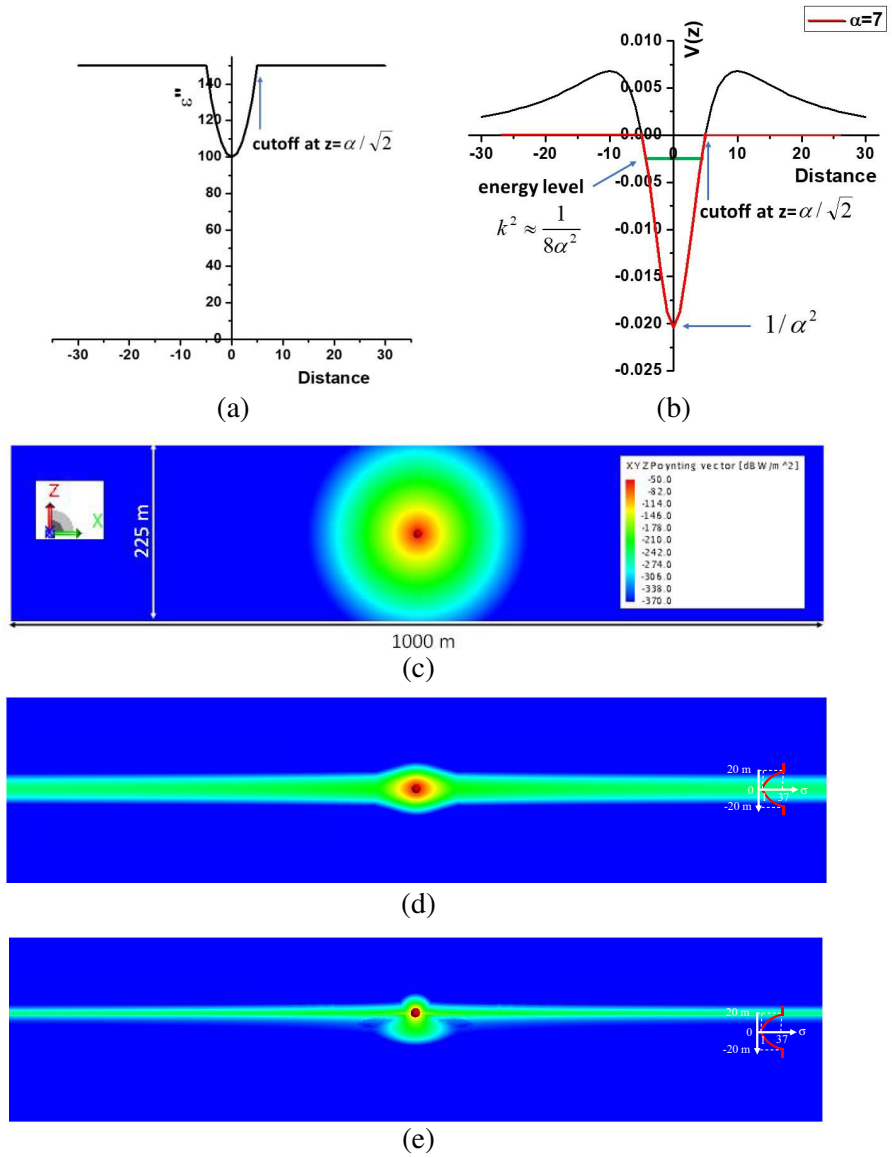

Figure 2. TM wave propagation in a one-layer configuration. (a) Spatial distribution of ε'' inside a "parabolic" conductive stratum defined as $\varepsilon = A + Bz^2$, where both A and B coefficients are large and imaginary, so that $A/B = \alpha^2$ is positive and real. In this example $A = 100i$ and $\alpha = 7$. The parabolic behavior is cut off at $z = \alpha/2^{1/2}$. (b) The effective potential energy $V(z)$ inside such a "parabolic" conductive stratum. When the potential well is cut off at $z = \alpha/2^{1/2}$, as indicated by the red line, the shallow energy level (shown in green) may be obtained analytically as $k^2 \approx 1/8\alpha^2$. (c) Numerical simulations of TM wave propagation away from a point dipole source in a homogeneous medium having conductivity $\sigma = 1\,\mathrm{S/m}$ (top). (d)–(e) Numerical simulations of TM wave propagation away from a point dipole source in a conductive stratum having a parabolic conductivity dependence $\sigma(z) = (1 + 0.1z^2)\,\mathrm{S/m}$ (where z is the distance in meters in the range $-19\,\mathrm{m} \le z \le 19\,\mathrm{m}$ (see inset)), sandwiched between infinite homogeneous media having $\sigma = 37.1\,\mathrm{S/m}$. Images (c)–(e) show maps of the total Poynting vector for the TM wave at 15 kHz and are in the same scale shown in Fig. 2(c). The point dipole source is placed in the center of the conductive stratum (d) or the homogenous medium 0.5 m away from the interface with the conductive stratum (e). Propagation length of the TM mode along the "parabolic" stratum considerably exceeds the conventional skin depth in a homogeneous medium.

gradient leads to much longer propagation range in the x direction, in spite of the overall increase in the conductivity value. Note that the medium conductivity in these examples ($\sigma \sim 1\,\mathrm{S/m}$) roughly corresponds to a typical conductivity of seawater [6]. For many applications it is crucial to consider boundary effects. Fig. 2(e) shows TM wave propagation away from the dipole point source placed in the homogeneous medium 0.5 m away from the conductive stratum layer. As can be seen from Fig. 2(e), the long range surface wave in this case propagates along the interface between homogeneous medium and the conductive stratum. The mode centered in the stratum is also visible but its intensity is lower than in Fig. 2(d), and it attenuates faster. Our numerical simulations confirm that electromagnetic waves in stratified conductive media may have propagating character, and that the propagation length of such waves may be considerably larger than the skin depth.

The fact that the system having high loss starts behaving as a low-loss low-dimensional system is non-trivial and quite remarkable. The physical origin of this seemingly paradoxical behavior is in fact quite straightforward. It may be traced back to the well-known effect of charge accumulation whenever there is a gradient of conductivity in a medium and a non-zero component of electric field parallel to it. In the electrostatic case the corresponding volumetric charge density ρ is obtained as

$$\rho = -\frac{\varepsilon_0 \nabla\sigma \cdot \vec{E}}{\sigma} \tag{15}$$

(see for example [8]). Therefore, at non-zero frequencies the obtained low loss TM wave solution of Maxwell equations may be characterized as a propagating wave of charge density. Note also that this wave is deeply subwavelength ($\lambda_{TM} \ll \lambda_0$), which means that a periodically stratified conductive medium, in which the conductivity distribution in each individual layer looks like in Fig. 2(a), should behave as a very high refractive index metamaterial. Based on Eq. (10), the effective refractive index in such a metamaterial in the x and y directions may be estimated as

$$n = \frac{\lambda_0}{\lambda_{TM}} \approx \frac{\lambda_0}{4\sqrt{2}\pi\alpha} \tag{16}$$

4. MULTILAYERED STRUCTURES

Since the properties of such periodically stratified media are of interest in many fields of science and engineering (e.g., in super-resolution optical microscopy, underground and underwater radio communication, plasma etc.) let us study these properties in more detail. In particular, let us determine the transmission properties of such a periodically stratified conductive media along z direction.

As an example, let us consider the following straightforward periodic extension of the parabolic distribution of the dielectric permittivity given by Eq. (4):

$$\varepsilon(z) = A\left(1 + \sin^2\frac{z}{\alpha}\right), \tag{17}$$

where $A \gg 1$ is an imaginary coefficient, and $\alpha \ll \lambda$ is real. The corresponding effective potential $V(z)$ for the TM wave is

$$V(z) \approx -\frac{4\pi^2 A}{\lambda_0^2}\left(1 + \sin^2\frac{z}{\alpha}\right) - \frac{\cos\dfrac{2z}{\alpha}}{\alpha^2 \sin^2\dfrac{z}{\alpha} + \alpha^2} + \frac{3\sin^2\dfrac{2z}{\alpha}}{4\alpha^2\left(1 + \sin^2\dfrac{z}{\alpha}\right)^2} \tag{18}$$

Once again, $\mathrm{Re}(V) \gg \mathrm{Im}(V)$ in the limit $\lambda \gg \alpha$. This effective potential is plotted in Fig. 3(a). Similar to Fig. 2(b), the regions of positive $V(z)$ have been cut off, so that we may use the same approximate energy level given by Eq. (6) in our analysis. According to the Bloch theorem [9], the solution of the effective Schrödinger Eq. (2), when the potential is periodic, can be written as:

$$\psi(z) = e^{ik_z z} u(z), \tag{19}$$

where $u(z)$ is a periodic function which satisfies $u(z) = u(z + \pi\alpha)$ — see [10]. Using the Born-von Karman boundary conditions $y(0) = y(M\pi\alpha)$, where M is the number of layers, results in the following quantization for k_z:

$$k_z = \frac{2}{M\alpha}m, \quad \text{where} \quad m = 0, \pm 1, ..., \pm\frac{M}{2} \tag{20}$$

In the limit $M \to \infty$ a continuous transmission band is formed for $0 \le k_z \le 1/\alpha$. The periodic function $u(z)$ may be expressed as a Fourier series:

$$u(z) = \sum\nolimits_m U_m e^{i2mz/\alpha} \tag{21}$$

On the other hand, the periodic potential $V(z)$ may also be expanded as a Fourier series as:

$$V(z) = \sum\nolimits_m V_m e^{i2mz/\alpha} \tag{22}$$

As a result, the Schrodinger equation may be re-written as

$$\left[\left(k_z + \frac{2m}{\alpha}\right)^2 + k^2\right] U_m + \sum\nolimits_{m'} V_{m'} U_{m-m'} = 0 \tag{23}$$

Using the tight binding approximation, its solution may be written approximately as

$$k^2 = k_0^2 - 2S\cos\left(\pi\alpha k_z\right), \tag{24}$$

where $k_0 \approx 1/2\sqrt{2}\alpha$ is the energy level of a single potential well given by Eq. (6), and S is the hopping integral $S \approx -k_0^2 \langle\psi_0|\psi_1\rangle$, which is calculated using the wave functions of the original potential well (Eq. (5)) centered at $z = 0$ and $z = \pi\alpha$ planes, respectively. Using the approximations $\psi_0 \sim e^{-|k_0 z|}$ and $\psi_1 \sim e^{-|k_0(z-\pi\alpha)|}$, the hopping integral may be estimated as

$$S \approx -\pi\alpha k_0^3 e^{-k_0\pi\alpha} \tag{25}$$

This analytical theory is supported by numerical simulations shown in Figs. 3(b)–(d). The conductivity profile used to produce these figures is a periodic stack of layers where each period consists of 10 cm thick layer of $\sigma = 1.5\,\mathrm{S/m}$ and 1.9 m thick layer of $\sigma = 1\,\mathrm{S/m}$. This periodic structure consists of 113 periods and is sandwiched between homogeneous medium having conductivity $\sigma = 1\,\mathrm{S/m}$. The radiating dipoles in these figures are oriented perpendicular to the layers. Figs. 3 and 4 demonstrate that introduction of the periodic conductivity variations in the transverse direction enables power flow in z-direction. In addition to the volumetric small-k wave and long propagating confined 2D mode (similar to Fig. 2), the point source (vertical electric dipole) also excites volumetric high-k waves (predicted by Eq. (24)) which manifest themselves as four perturbances emanated from the central circle (see Fig. 3(b) and Fig. 3(d)). The difference between low-k and high-k 3D modes is especially clear on Fig. 3(d) showing Poynting vector distribution in X-Y cut. The inset in the center shows the corresponding phase of E_x component of electric field. It clearly indicates the difference in wave numbers of these two 3D modes. The high-k mode attenuates faster than the confined 2D mode due to its volumetric 3D character, but still can propagate longer than the small-k wave. The beam propagating in the x-y plane becomes considerably broader in z-direction. The complicated interference pattern revealed by Fig. 3(c) is a manifestation of the fact that the wavelength of the volumetric high-k modes becomes comparable to the period of the stratified medium. In addition, the distribution of x-component of the Poynting vector has well pronounced beam splitting typical, for example, for hyperbolic media [13]. By comparing Figs. 3(b) and 3(c), one can see that z-component of the Poynting vector makes a significant contribution to the total magnitude. This is mostly related to the vertex nature of the excited field, rather than with loss during propagation along x direction. When a single point dipole source is replaced with a periodic array of sources as shown in Fig. 4, the resulting TM mode structure looks even broader and becomes even closer to the analytical model predictions.

It is also interesting to note that somewhat related effects may be obtained in the effective medium theory limit while analyzing the properties of multilayer metal-dielectric structures [14]. Using the Maxwell-Garnett approximation, the dielectric tensor components of such a multilayer "metamaterial" may be written as follows:

$$\varepsilon_{x,y} = n\varepsilon_m + (1-n)\,\varepsilon_d \tag{26}$$

$$\varepsilon_z = \frac{\varepsilon_m \varepsilon_d}{(1-n)\,\varepsilon_m + n\varepsilon_d} \tag{27}$$

where n is the volume fraction of metal, and ε_m and ε_d are the dielectric permittivities of the metal and dielectric, respectively [15]. In the limit $\varepsilon_m \gg \varepsilon_d$, the z component of the dielectric tensor is real

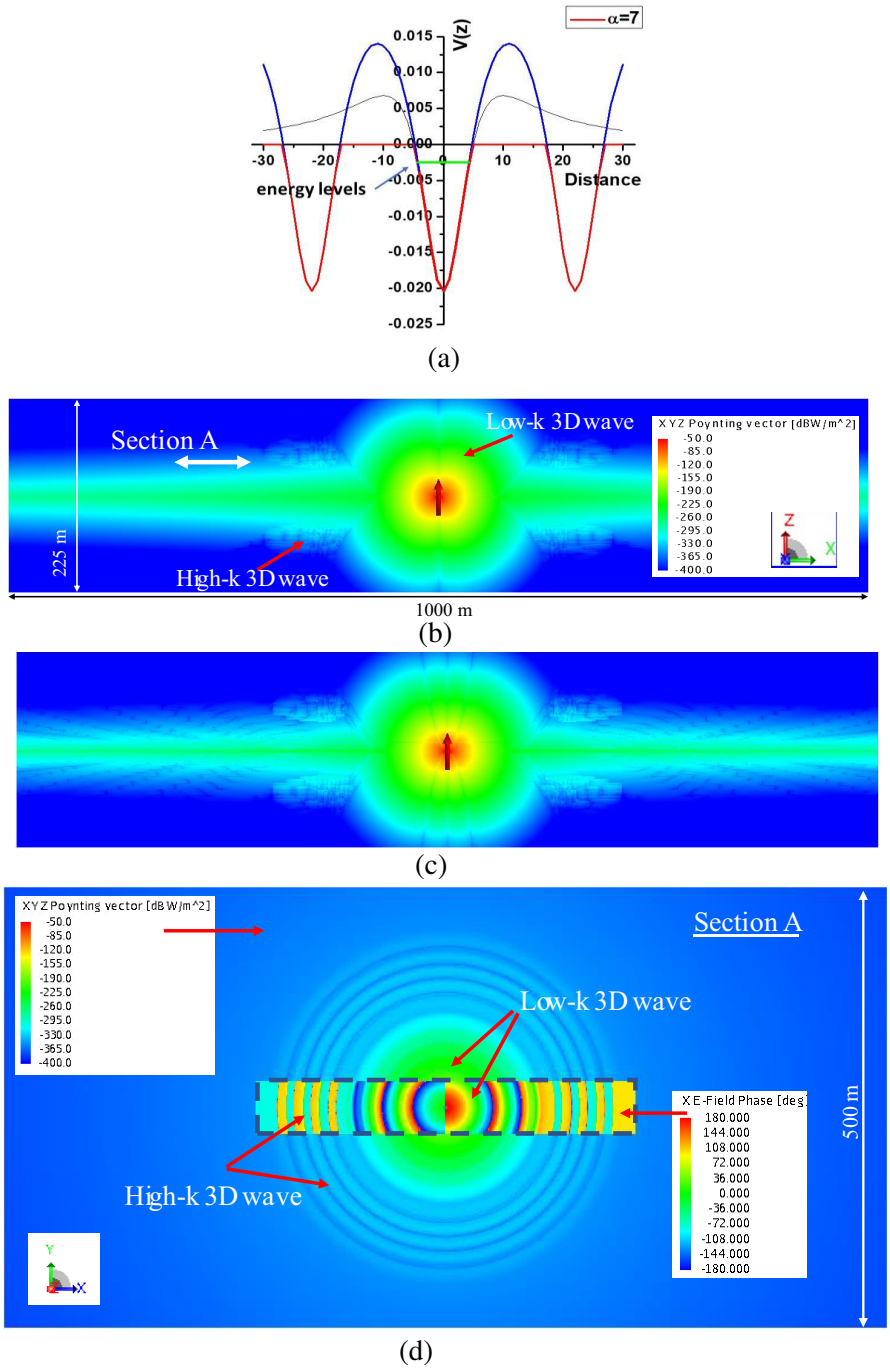

Figure 3. TM wave propagation in a periodic conductive multi-layer configuration. (a) The periodic dielectric constant is defined as $\varepsilon(z) = A(1 + \sin^2(z/\alpha))$. Similar to Fig. 2(b), the positive sections of the periodic potential well are cut off, as indicated by the red line. (b), (c), (d) Numerical simulations of TM wave propagation along such a multilayer conductive stratum geometry. The wave is excited by a single point dipole indicated by the red arrow. The width of the central beam visible in the maps of the total Poynting vector (b) and its x-component (c) is considerably broader compared to the central beam in a single stratum shown in Fig. 2(c). (d) The total Poynting vector distribution in X-Y cut made 44 m above the dipole source. The inset in the center shows the corresponding phase of E_x component of electric field. Images (b)–(d) are plotted in the same scale shown in Fig. 3(b).

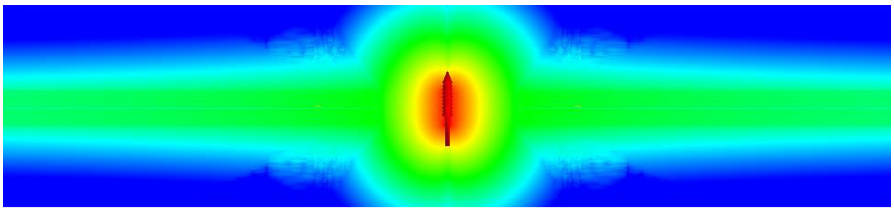

Figure 4. The total Poynting vector of TM wave excited in the same structure by a periodic configuration of 10 point dipoles (one per period). The scale, size and orientation of the plane are the same as in Figs. 3(b) and (c).

and positive: $\varepsilon_z \approx \varepsilon_d/(1-n)$, which results in existence of long-distance propagating modes within the "hyperbolic" frequency bands inside such a "metamaterial", which is mostly made of non-transparent metal. However, we must point out that a dramatic difference between our results and the hyperbolic media example is that hyperbolic media are made using low loss dielectrics as one of their components.

In a somewhat similar fashion, a single layer structure depicted in Fig. 2 supports a single frequency-dependent propagating mode which is defined by the eigenstate of the one-dimensional effective Schrodinger equation (Eq. (2)). In the particular case which is solved analytically in our manuscript (see Eqs. (4)–(6)), the dispersion law $\omega(k)$ of this mode is defined by the dispersion of the frequency-dependent parameter α, which in tern is determined by the frequency-dependent $\varepsilon(\omega)$ via Eg. (4). In the case of the multilayer structures depicted in Fig. 3, the single mode defined by Eq. (6) becomes a band, which is described by Eq. (24). This behaviour is in fact quite similar to the behaviour of the multilayer metal-dielectric structures discussed above, in which a plasmonic band of a single metal layer becomes a "hyperbolic band" of the multilayer hyperbolic metamaterial.

5. CONCLUSIONS

In conclusion, we have demonstrated that contrary to common beliefs, electromagnetic waves may propagate through some lossy conductive media. Typically, such media are characterized by non-Hermitian Hamiltonians having complex eigenvalue spectrum, which results in strong wave attenuation. It has been recently demonstrated however that a non-Hermitian system may have real eigenvalue spectrum if such a system exhibits PT-symmetry [11]. Usually, the real spectrum leading to long-range wave propagation in such systems is enabled by engineered counterplay between loss and gain [5]. The fundamental importance of our findings consists in the demonstration of a new class of electromagnetic media with inherently high dissipation, no gain and no PT-symmetry, which nevertheless has almost real eigenvalue spectrum, and which supports propagating electromagnetic waves. The non-trivial non-perturbative character of these newly found propagating electromagnetic waves is revealed by the fact that unlike conventional wave-like solutions of source-free Maxwell equations, these waves completely disappear in the lossless limit. The very existence of these newly found highly non-trivial electromagnetic waves depends on the presence of very high losses ($\varepsilon'' \gg \varepsilon'$).

Our findings have broad implications in many fields of science and engineering. They enable radio communication and imaging through conductive media, such as seawater [6], various soils, plasma and biological tissues [3]. For example, since natural stratification is often observed in many underground sedimentary rocks and soils (as illustrated for example in Fig. 1(b)) and these rocks and soils typically have $\varepsilon'' \gg \varepsilon'$ at radio frequencies, using our theoretical results it may become possible to greatly improve spatial resolution and ground penetrating performance of the ground penetrating radar (GPR) techniques. Our findings may also enable novel super-resolution microscopy techniques and lower-loss electromagnetic metamaterial designs working across such previously inaccessible frequency ranges as deep UV, in which all the conventional optical materials suffer from very large losses [12]. Compared to the earlier results reported in [3, 12] where the propagation length of the surface waves remained similar (or even below) the skin depth, the findings reported here are quite novel and striking, since several analytically solvable model distributions of $\varepsilon(z)$ have been found which give rise to electromagnetic waves propagating in highly lossy media over distances which greatly exceed the conventional skin depth.

REFERENCES

1. Blum, W. E. H., P. Schad, and S. Nortcliff, *Essentials of Soil Science*, Borntraeger Science Publishers, Stuttgart, 2018.
2. Vance, S., M. Bouffard, M. Choukroun, and C. Sotin, "Ganymede's internal structure including thermodynamics of magnesium sulfate oceans in contact with ice," *Planetary and Space Science*, Vol. 96, 62–70, 2014.
3. Smolyaninov, I. I., "Surface electromagnetic waves at gradual interfaces between lossy media," *Progress In Electromagnetics Research*, Vol. 170, 177–186, 2021.
4. Shelby, R. A., D. R. Smith, and S. Schultz, "Experimental verification of a negative index of refraction," *Science*, Vol. 292, 77–79, 2001.
5. Guo, A., G. J. Salamo, D. Duchesne, R. Morandotti, M. Volatier-Ravat, V. Aimez, G. A. Siviloglou, and D. N. Christodoulides, "Observation of PT-symmetry breaking in complex optical potentials," *Phys. Rev. Letters*, Vol. 103, 093902, 2009.
6. Smolyaninov, I. I., Q. Balzano, C. C. Davis, and D. Young, "Surface wave based underwater radio communication," *IEEE Antennas and Wireless Propagation Letters*, Vol. 17, 2503–2507, 2018.
7. Landau, L. D. and E. M. Lifshitz, *Quantum Mechanics*, Elsevier, 1977.
8. Li, Y. and D. W. Oldenburg, "Aspects of charge accumulation in DC resistivity experiments," *Geophysical Prospecting*, Vol. 39, 803–826, 1991.
9. Bloch, F., "Über die quantenmechanik der elektronen in kristallgittern," *Zeitschrift für Physik*, Vol. 52, 555–600, 1929.
10. Kittel, C., *Introduction to Solid-state Physics*, 173–196, John-Wiley, Singapore, 1996.
11. Bender, C. M. and S. Boettcher, "Real spectra in non-Hermitian Hamiltonians having PT Symmetry," *Phys. Rev. Letters*, Vol. 80, 5243, 1998.
12. Smolyaninov, I. I., "Gradient-index nanophotonics," *Journal of Optics*, Vol. 23, 095002, 2021.
13. Kozyrev, A. B., C. Qin, I. V. Shadrivov, Yu. S. Kivshar, I. L. Chuang, and D. W. van der Weide, "Wave scattering and splitting by magnetic metamaterials," *Opt. Express*, Vol. 15, 11714–11722, 2007.
14. Smolyaninov, I. I., *Hyperbolic Metamaterials*, Morgan & Claypool/Institute of Physics, London, 2018.
15. Wangberg, R., et al., "Nonmagnetic nanocomposites for optical and infrared negative-refractive-index media," *J. Opt. Soc. Am. B*, Vol. 23, 498, 2006.